LEARNING DIRICHLET KERNEL HISTOGRAM FUNCTIONS FOR PATTERN RECOGNITION

Koichi Niijima

Kyushu University
1-10-6, Hakozaki, Higashi-ku, 812-8581, Fukuoka, Japan
email: niijima@i.kyushu-u.ac.jp

ABSTRACT

A formula of approximating histograms is presented. The formula is an explicit function of data permitting the inclusion of unknown parameters. The parameters in the formula are learned so as to classify training data to build a pattern classifier. Recognition is performed by applying the classifier to testing data. Our method is used for the recognition of vehicle-type.

1. INTRODUCTION

Histograms have been widely used in pattern recognition. They are robust to noise and local image transformations. Histograms were initially applied to the identification of 3-D objects [12]. Following that work, a recognition system based on histograms was proposed [11]. These papers use color effectively, therefore, their approaches seem to be insufficient for the discrimination of greylevel images. We also have a problem that histograms do not capture spatial image information. To remedy such a deficiency, Hadjidemetriou *et al.* [2, 3, 4] proposed a multiresolution histogram method. Their approach constructs a feature vector of an image from the difference histograms proportional to the discrete Fisher information measures, computed from the multiresolution histograms of the image. They performed pattern recognition by comparing these feature vectors. Recently, their method has been applied to the classification of mammographic densities [6]. In that work, the feature vectors constructed from multiresolution histograms were classified using a multiclass directed acyclic graph and a support vector machine. However, satisfactory recognition results have not been obtained yet.

In this paper, we present a formula of approximating histograms, which is an explicit function of data permitting the inclusion of unknown parameters. The data containing unknown parameters are constructed by applying the lifting dyadic wavelet transform to an image. We produce a histogram function corresponding to each of such data. The unknown parameters are learned so as to separate the constructed histogram functions to build a pattern classifier. Since our method controls the histogram functions actively, the obtained classifier can be a powerful tool for pattern recognition. In simulation, the proposed method is used to solve a vehicle-type recongnition problem, and the results of recognition are compared with those of the multiresolution histogram technique.

2. DIRICHLET KERNEL HISTOGRAM FORMULA

We derive a formula of approximating histograms, which is called a Dirichlet kernel histogram formula, to utilize it for pattern recognition. Let N be a positive integer, and divide the interval $[-1,1]$ into $2N+1$ equidistant subintervals $[\xi_n,\xi_{n+1}]$. Here, ξ_n represent $\xi_n=(2n-1)/(2N+1)$, $n=-N,...,N+1$. The midpoint of $[\xi_n,\xi_{n+1}]$ is given by $t_n=2n/(2N+1)$. Let us denote M data by z_m, $m=0,...,M-1$. The datasize M may be distinct per data. The data z_m are normalized as $-1\le z_m\le 1$. Let $\bar{z}_m$ be a representative of z_m existing in the subinterval $[\xi_n,\xi_{n+1}]$. The histogram $\bar{f}_n$ of z_m is the number of $\bar{z}_m$ appearing in $[\xi_n,\xi_{n+1}]$.

The following theorem holds.

Theorem 1 ([10]). The ratio of histogram $\bar{f}_n$ to M can be approximated by

$$f(t;\mathbf{z})=\frac{1}{(2N+1)M}\sum_{m=0}^{M-1}\left(1+2\sum_{k=1}^{N}\cos\pi k(z_m-t)\right)$$
$$=\frac{1}{(2N+1)M}\sum_{m=0}^{M-1}\frac{\sin(N+\frac{1}{2})\pi(z_m-t)}{\sin\frac{1}{2}\pi(z_m-t)},\qquad -1\le t\le 1, \quad (1)$$

where $\mathbf{z}=(z_0,...,z_{M-1})$.

The outline of proof is described as follows: We apply the discrete Fourier transform to the histogram $\bar{f}_n$, and transform it using a moment relation between $\bar{f}_n$ and $\bar{z}_m$. The histogram $\bar{f}_n$ is obtained by exploiting the inverse discrete Fourier transform. As a result, we have $\bar{f}_n=Mf(t_n;\bar{\mathbf{z}})$ with $\bar{\mathbf{z}}=(\bar{z}_0,...,\bar{z}_{M-1})$. This means that $f(t;\mathbf{z})$ is an approximation of $\bar{f}_n/M$.

Since $f(t;\mathbf{z})$ in Theorem 1 is a Dirichlet kernel function when $z_m=0$, we call it a Dirichlet kernel histogram (Dkh) formula or a Dkh function. It is important to notice that the Dkh formula $f(t;\mathbf{z})$ is an explicit function of the data z_m, $m=0,...,M-1$. Of course, z_m may include unknown parameters. Since $\int_{-1}^{1}f(t;\mathbf{z})dt=2/(2N+1)$ does not depend on M, we can compare the Dkh functions with different datasizes.

Using the first equation of (1), we obtain

Corollary 1. The L^2-distance between two Dkh functions $f(t;\mathbf{z}^\nu)$ with $\mathbf{z}^\nu=(z_0^\nu,...,z_{M_\nu-1}^\nu)$, $\nu=1,2$, is given by

$$\|f(\cdot;\mathbf{z}^1)-f(\cdot;\mathbf{z}^2)\|^2=\int_{-1}^{1}(f(t;\mathbf{z}^1)-f(t;\mathbf{z}^2))^2dt$$
$$=\frac{4}{(2N+1)^2}\sum_{k=1}^{N}\left((a^1[k]-a^2[k])^2+(b^1[k]-b^2[k])^2\right).$$

Here, $a^\nu[k]$ and $b^\nu[k]$ denote

$$a^\nu[k] = \frac{1}{M_\nu}\sum_{m=0}^{M_\nu-1}\cos(k\pi z_m^\nu), \qquad b^\nu[k] = \frac{1}{M_\nu}\sum_{m=0}^{M_\nu-1}\sin(k\pi z_m^\nu),$$

respectively.

Corollary 1 will be used to derive a classification algorithm.

3. LIFTING SCHEME

To obtain image data including free prameters, we use a set of lifting dyadic wavelet filters:

$$h_n = h_n^o, \tag{2}$$
$$g_n = g_n^o - \sum_l \lambda_l h_{n-l}^o, \tag{3}$$
$$\tilde{h}_n = \tilde{h}_n^o + \sum_l \lambda_{-l}\tilde{g}_{n-l}^o, \qquad \tilde{g}_n = \tilde{g}_n^o,$$

where λ_l's are free parameters. Here, $\{h_n^o, g_n^o, \tilde{h}_n^o, \tilde{g}_n^o\}$ denotes a set of old dyadic wavelet filters, in which h_n^o and g_n^o are low-pass and high-pass analysis filters, respectively, and $\tilde{h}_n^o$ and $\tilde{g}_n^o$ low-pass and high-pass synthesis filters, respectively. It can be shown that the above lifting wavelet filters also become dyadic wavelet filters ([5]). In this paper, only (2) and (3) will be exploited. Images are not subsampled by these analysis filters. From now on, a sequence of free parameters is restricted to a finite sequence.

Let $u_{i,j}$ denote an original image. Applying the filter (2) to $u_{i,j}$ in vertical direction, and the lifting filter (3) to the resulting components in horizontal direction, we obtain

$$D_{i,j} - \sum_{l=-L}^{L}\lambda_l^d C_{i+l.j}. \tag{4}$$

Here, $C_{i,j} = \sum_{k,m} h_k^o h_m^o u_{i+k,j+m}$ represent low-pass components, $D_{i,j} = \sum_{k,m} g_k^o h_m^o u_{i+k,j+m}$ high-pass components in horizontal direction, and λ_l^d's free parameters in horizontal direction. Next, we apply the filter (2) to $u_{i,j}$ in horizontal direction, and the lifting filter (3) to the resulting components in vertical direction to get

$$E_{i,j} - \sum_{l=-L}^{L}\lambda_l^e C_{i.j+l}, \tag{5}$$

where $E_{i,j} = \sum_{k,m} h_k^o g_m^o u_{i+k,j+m}$ are high-pass components in vertical direction, and λ_l^e's free parameters in vertical direction. Adding (4) and (5) yields the components

$$v_{i,j} = D_{i,j} + E_{i,j} - \sum_{l=-L}^{L}\lambda_l^d C_{i+l.j} - \sum_{l=-L}^{L}\lambda_l^e C_{i.j+l}. \tag{6}$$

Note that $v_{i,j}$ has the information of original image $u_{i,j}$ around (i,j), because $C_{i+l.j}$ and $C_{i.j+l}$ in (6) have it.

The lifted components (6) have been used for developing facial parts detection systems [7, 8, 13]. They have also been exploited for the development of person authentication systems [9, 14].

In this paper, the components $v_{i,j}$ of (6) are normalized to construct a Dkh function. Although the maximum of $v_{i,j}$ cannot be calculated in advance, because (6) include unknown parameters, they can formally be normalized as

$$w_{i,j} = \frac{v_{i,j} - \bar{v}}{\max_{(i,j)\in\Omega}|v_{i,j} - \bar{v}|}, \tag{7}$$

where Ω denotes an image region of $v_{i,j}$, and $\bar{v}$ an average of $v_{i,j}$ in Ω. The Dkh function for $w_{i,j}$ takes the following form.

$$f(t;\mathbf{w}) = \frac{1}{(2N+1)\#\Omega}\sum_{(i,j)\in\Omega}\left(1+2\sum_{k=1}^{N}\cos\pi k(w_{i,j}-t)\right)$$
$$= \frac{1}{(2N+1)\#\Omega}\sum_{(i,j)\in\Omega}\frac{\sin(N+\frac{1}{2})\pi(w_{i,j}-t)}{\sin\frac{1}{2}\pi(w_{i,j}-t)},$$
$$-1 \le t \le 1. \tag{8}$$

Here $\mathbf{w} = (w_{i,j})$, $(i,j)\in\Omega$, where $\#\Omega$ denotes the number of pixels of $w_{i,j}$.

4. CLASSIFIER

4.1 Learning of free parameters

Suppose that there are S classes of images. The ν-class consists of T training images $u_{i,j}^{\tau,\nu}$, $\tau = 1,...,T$. We construct the components $w_{i,j}^{\tau,\nu}$ of the form (7) from $u_{i,j}^{\tau,\nu}$ going through the lifting (6) and the normalization (7). Furthermore, we construct the Dkh functions $f(t;\mathbf{w}^{\tau,\nu})$ having the form (8) from $w_{i,j}^{\tau,\nu}$. The next task is to calculate the average of the Dkh functions in ν-class as

$$\bar{f}^\nu(t) = \frac{1}{T}\sum_{\tau=1}^{T} f(t;\mathbf{w}^{\tau,\nu}),$$

and the total average of the Dkh functions as

$$\bar{f}(t) = \frac{1}{S}\sum_{\nu=1}^{S}\bar{f}^\nu(t).$$

Notice that the free parameters are included also in these averages. We use the discriminant analysis method to learn the parameters. The method in the present case is described as follows: Determine the parameters $\lambda^d = (\lambda_{-L}^d,...,\lambda_L^d)$ and $\lambda^e = (\lambda_{-L}^e,...,\lambda_L^e)$ so as to minimize the functional

$$J(\lambda^d,\lambda^e) = \frac{\sum_{\nu=1}^{S}\sum_{\tau=1}^{T}\|f(\cdot;\mathbf{w}^{\tau,\nu}) - \bar{f}^\nu\|^2}{\sum_{\nu=1}^{S}\|\bar{f}^\nu - \bar{f}\|^2}, \tag{9}$$

where $\|\cdot\|$ denotes the L^2-norm. The norms included in (9) can be computed using Corollary 1 as

$$\|f(\cdot;\mathbf{w}^{\tau,\nu}) - \bar{f}^\nu\|^2$$
$$= \frac{4}{(2N+1)^2}\sum_{k=1}^{N}\left((a^{\tau,\nu}[k] - \bar{a}^\nu[k])^2 + (b^{\tau,\nu}[k] - \bar{b}^\nu[k])^2\right),$$

$$\|\bar{f}^\nu - \bar{f}\|^2 = \frac{4}{(2N+1)^2}\sum_{k=1}^{N}\left((\bar{a}^\nu[k] - \bar{a}[k])^2 + (\bar{b}^\nu[k] - \bar{b}[k])^2\right).$$

Here, $a^{\tau,v}[k]$ and $b^{\tau,v}[k]$ indicate

$$a^{\tau,v}[k] = \frac{1}{\#\Omega_{\tau,v}} \sum_{(i,j)\in\Omega_{\tau,v}} \cos(k\pi w_{i,j}^{\tau,v}),$$

$$b^{\tau,v}[k] = \frac{1}{\#\Omega_{\tau,v}} \sum_{(i,j)\in\Omega_{\tau,v}} \sin(k\pi w_{i,j}^{\tau,v}),$$

respectively, where $\#\Omega_{\tau,v}$ denotes the number of pixels of $u_{i,j}^{\tau,v}$. Also, we put $\bar{a}^v[k] = \sum_{\tau=1}^{T} a^{\tau,v}[k]/T$, $\bar{b}^v[k] = \sum_{\tau=1}^{T} b^{\tau,v}[k]/T$, $\bar{a}[k] = \sum_{v=1}^{S} \bar{a}^v[k]/S$, and $\bar{b}[k] = \sum_{v=1}^{S} \bar{b}^v[k]/S$.

To apply a minimization method to $J(\lambda^d, \lambda^e)$, we have to differentiate it with respect to λ_l^d and λ_l^e, and thus with respect to $w_{i,j}^{\tau,v}$. However, since the denominator of $w_{i,j}^{\tau,v}$ is non-differentiable, differentiation is done only for the numerator.

4.2 Inverse problems

The present minimization problem is considered as a discrete inverse problem of elliptic-type of partial differential operators. To explain this, we return to (6). If choosing the high-pass filter g_n^o as $g_0^o = -0.25$, $g_1^o = 0.5$, $g_2^o = -0.25$, and $g_n^o = 0.0$ otherwise, which is a kind of dyadic wavelet filters, the filter g_n^o becomes the discrete Laplacian operator. Therefore, a continuous version of (6) can be written as

$$v(x,y) = -\left(\frac{\partial^2}{\partial x^2}(I_y u)(x,y) + \frac{\partial^2}{\partial y^2}(I_x u)(x,y)\right) - I(\lambda^d, \lambda^e)u(x,y). \qquad (10)$$

Here I_y, I_x and $I(\lambda^d, \lambda^e)$ represent the integral operators defined by

$$(I_y u)(x,y) = \int h^o(y')u(x,y+y')dy',$$

$$(I_x u)(x,y) = \int h^o(x')u(x+x',y)dx',$$

$$(I(\lambda^d, \lambda^e)u)(x,y) = \sum_{l=-L}^{L} \left(\lambda_l^d C(x+l,y) + \lambda_l^e C(x,y+l)\right),$$

respectively, where $h^o(x)$ is a continuous version of low-pass filter h_n^o, and $C(x,y) = \int\int h^o(x')h^o(y')u(x+x',y+y')dx'dy'$. Learning λ^d and λ^e by our method is regarded as solving a discrete inverse problem of the elliptic-type of partial differential operator (10).

Such inverse problems generally become ill-posed. Therefore, stabilization is needed, and is often executed by using the Tikhonov's regularization method. The method is to add the penalty term

$$\sum_{l=-L}^{L} ((\lambda_l^d)^2 + (\lambda_l^e)^2)$$

to $J(\lambda^d, \lambda^e)$ of (9), and to minimize

$$J(\lambda^d, \lambda^e) + P \sum_{l=-L}^{L} ((\lambda_l^d)^2 + (\lambda_l^e)^2),$$

where P denotes a penalty constant. This fact was pointed out also in [7].

5. RECOGNITION METHOD

Recognition is performed by comparing a Dkh function for a testing image with the Dkh average functions for training images. First, we compute Dkh functions for training images and their average functions per class by using the learned parameters. Next, a Dkh function for a testing image is computed by exploiting the same parameters. We measure the L^2-distances between the Dkh function and the Dkh average functions for training images. The testing image is judged to be in v-class, if its Dkh function is nearest to the Dkh average function of v-class.

6. RECOGNITION OF VEHICLE-TYPE

We consider a problem of recognizing vehicle-type. The types of vehicles are bus, truck, van, mini-car, and sedan. Using a webcamera, we took the pictures of vehicles going at a speed of about 40km/h on a road, and cut off only moving objects. The values of background areas are almost zero. Each image has a size of 64×64. The object is not always centered in an image, and is lacked partly in many examples. The captured images contain the shadow of a vehicle and, in some cases, walking people as noise. We captured 40 vehicles per type, therefore, the total number of samples is 200. About half of vehicles in each type is facing to the left, and the remaining to the right. From each type of vehicles, 10 vehicles are chosen for the use of training images, i.e., $T = 10$, and the remaining 30 images to use as testing images. Figure 1 shows a part of training images, and Fig. 2 a part of testing images.

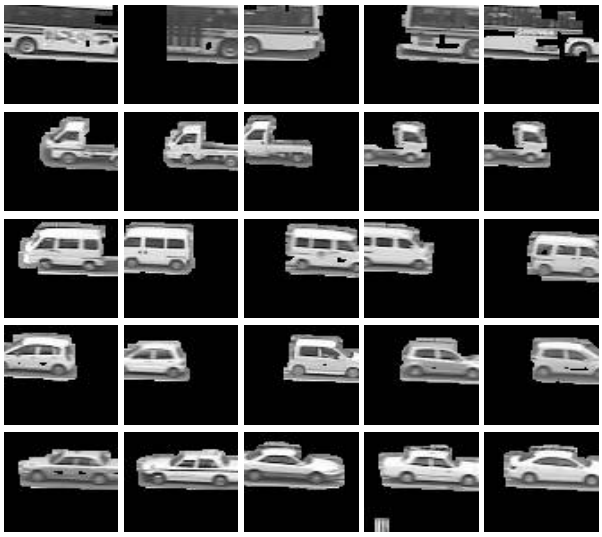

Figure 1: A part of training images; from the top of each line, bus, truck, van, mini-car, and sedan are arranged.

6.1 Our method

By the use of dichotomy, we separate 50 training images, each type of vehicles consists of 10 images. The free parameters λ_l^d's and λ_l^e's included in (7) are learned by our method so as to distinguish, first, bus and the other types of vehicles, second, truck and the other types of vehicles except for bus, thirdly, van and the remaining two types of vehicles, and last, mini-car and sedan. That is, we construct four classifiers,

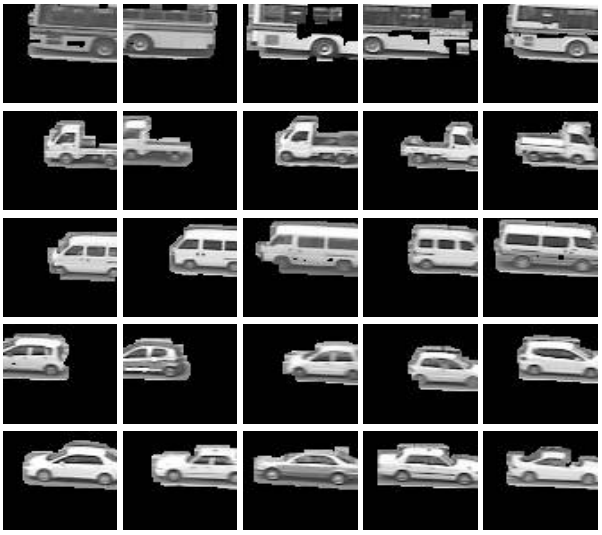

Figure 2: A part of testing images; from the top of each line, bus, truck, van, mini-car, and sedan are arranged.

which are tools for recognizing bus, truck, van, mini-car, and sedan. In all the cases, the number of free parameters in each direction is chosen as $2L+1=25$, i.e., $L=12$, and the number of mesh points of a Dkh function as $2N+1=11$, i.e., $N=5$. To ignore the background area in an original image, we use only the values of image exceeding some thresholds.

For recognition, we compute the Dkh functions having the form (8) for training images by using the parameters learned for the bus classifier, the truck classifier, the van classifier, and the mini-car classifier. Furthermore, the averages of these Dkh functions are calculated per vehicle-type. Figures through 3 to 6 illustrate the averages of Dkh functions for four classifiers.

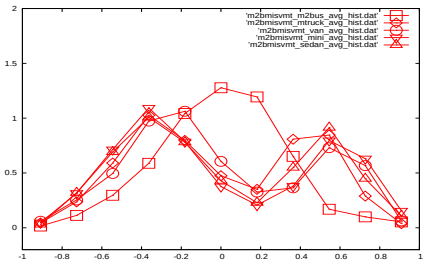

Figure 3: The averages of Dkh functions learned for training images of bus, truck, van, mini-car, and sedan.

In Fig. 3, the bus average function behaves like a Gaussian distribution with $t=0.0$ as a center, while the other ones have valleys near $t=0.0$. This suggests that bus is separable from the other types of vehicles. Figure 4 shows that the truck average function has a minimum around $t=-0.2$, however, the remaining average functions present sharp peaks there. Therefore, it is expected that only truck will be distinguishable from the remaining types of vehicles except for bus. Figure 5 presents a nortable difference between the van average function and the other ones in the interval $[-0.7,0.0]$. This expects that van will be separated from mini-car and sedan. Figure 6 shows that the average

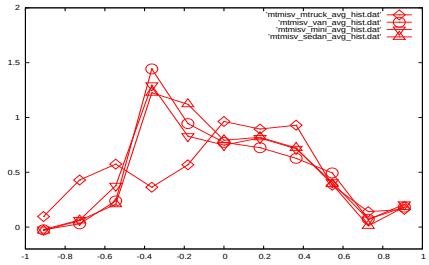

Figure 4: The averages of Dkh functions learned for training images of truck, van, mini-car, and sedan.

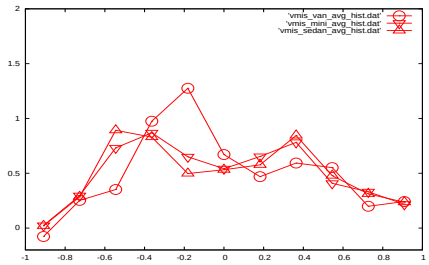

Figure 5: The averages of Dkh functions learned for training images of van, mini-car, and sedan.

function of mini-car is distinct from that of sedan in the interval $[-0.3,0.1]$, which hints the separability of them.

We examine the recognition ability of our method for 50 training images already used for learning, and for 150 testing images. The proposed method is evaluated by comparing the L^2-distances between a Dkh function for a training or testing image and the Dkh average functions obtained for the training images. If a Dkh function for an input image has the shortest distance from the bus Dkh average function in the bus classifier, the image is judged as bus. If not so, it is checked for the remaining classifiers. The results of recognition by our method are shown in Table 1 for the training and testing images. The agreement based on our method was 100% for the training images, and agreement obtained for the testing images was 90%.

6.2 Multiresolution histogram technique

For comparison, the experiments of vehicle-type recognition are performed by the use of the multiresolution histogram technique [4]. Although the method employs a Gaussian

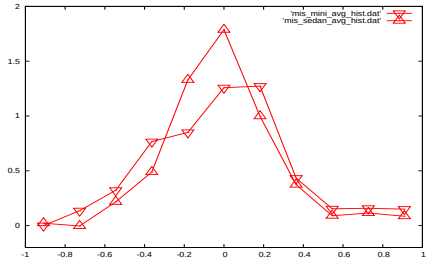

Figure 6: The averages of Dkh functions learned for training images of mini-car and sedan.

Table 1: Results of recognition by our method. b: bus, t: truck, v: van, m: mini-car, s: sedan.

	Training images					Testing images				
	b	t	v	m	s	b	t	v	m	s
b	10	0	0	0	0	24	2	4	0	0
t	0	10	0	0	0	0	28	0	2	0
v	0	0	10	0	0	0	0	30	0	0
m	0	0	0	10	0	0	2	0	27	3
s	0	0	0	0	10	0	0	0	2	28

pyramid of subsampled type to obtain histogram information, we use the dyadic wavelet transform not subsampled, because the size of images is small. Following the multiresolution histogram method, histograms proportional to the discrete Fisher information measures are computed for the training and testing images treated in Section 6. These histograms are concatenated to form a feature vector. We compare the L^1-distances between a feature vector for a training or testing image and the averages of the feature vectors for training images, and judge a viehicle-type with the shortest distance. Table 2 shows the results of recognition. The matching rate

Table 2: Results of recognition by the multiresolution histogram method. b: bus, t: truck, v: van, m: mini-car, s: sedan.

	Training images					Testing images				
	b	t	v	m	s	b	t	v	m	s
b	8	0	0	2	0	16	4	1	3	6
t	1	9	0	0	0	2	27	0	0	1
v	0	0	8	2	0	0	0	23	5	2
m	0	0	0	10	0	0	2	4	19	5
s	0	0	0	1	9	0	2	1	1	26

of the multiresolution histogram technique was 88% for the training images, while it was 74% for the testing images.

7. CONCLUSION AND FUTURE WORKS

We have proposed a pattern recognition method based on a Dkh formula. This formula is an explicit function of data permitting the inclusion of unknown parameters. By learning the parameters, we can build histogram pattern classifiers. Practically, free parameters in the Dkh functions constructed from the vehicle training images were learned by using the discriminant analysis method to produce a vehicle-type classifier. The experimental results show the high recognition ability of our method.

The proposed Dkh formula has many applications as well as pattern recognition. One of important problems is to find out a relation between our Dkh formula and the zero-norm investigated recently by Donoho's group [1]. Our Dkh function is considered as a generalization of Donoho's zero-norm, and differentiable with respect to data unlike the zero-norm. The Dkh formula can also be utilized for the control of strategy parameters included in solutions to evolution equations. These are future works.

Acknowledgments This work has been supported by a Monka-shoo Grant, which was obtained by Prof. M.T. Nakao in the Department of Mathematics at Kyushu University.

REFERENCES

[1] A.M. Bruckstein, D.L. Donoho, and M. Elad, "From sparse solutions of systems of equations to sparse modeling of signals and images," *SIAM Review*, vol.51, no.1, pp.34–81, 2009.

[2] E. Hadjidemetriou, M.D. Grossberg, and S.K. Nayar, "Histogram preserving image transformations," *Int'l Journ. Computer Vision*, vol.45, no.1, pp.5–23, 2001.

[3] E. Hadjidemetriou, M.D. Grossberg, and S.K. Nayar, "Spatial information in multiresolution histograms," *Proc. Computer Vision and Pattern Recognition Conf.*, vol.1, pp.702–709, 2001.

[4] E. Hadjidemetriou, M.D. Grossberg, and S.K. Nayar, "Multiresolution histograms and their use for recognition," *IEEE Trans. Pattern Analysis and Machine Intelligence*, vol.26, no.7, pp. 831–847, 2004.

[5] S. Mallat, *A Wavelet Tour of Signal Processing*. San Diego CA: Academic Press, 1998.

[6] I. Muhimmah and R. Zwiggelaar, "Mammographic density classification using multiresolution histogram information," *Proc. of the Int'l Special Topic Conf. on Information Technology in Biomedicine*, Mammography, 2006.

[7] K. Niijima, "Fast objects detection by variance-maximization learning of lifting wavelet filters," *Proc. Signal Processing with Adaptive Sparse Structured Representations (SPARS'05)*, pp.25–28, 2005.

[8] K. Niijima, "Facial parts recognition using lifting wavelet filters learned by kurtosis-minimization," *Proc. of Int'l Conf. on Computer Vision Theory and Applications (VISAPP'06)*, pp.41–47, 2006.

[9] K. Niijima, "Person authentication using learned parameters of lifting wavelet filters," *5th Int'l Workshop on Information Optics (WIO'06), AIP Conf. Proc.*, vol.860, pp.253-262, 2006.

[10] K. Niijima, "Recognition equipment, recognition method, program, and storage medium," *applied to the Japanese Patent Office for a patent*, no.2007-186304, July 17, 2007.

[11] M. Stricker and M. Orengo, "Similarity of color images," *Proc. SPIE Conf. Storage and Retrieval for Image and Video Databases III*, vol.2420, pp.381–392, 1995.

[12] M.J. Swain and D.H. Ballard, "Color Indexing," *Int'l Journ. of Computer Vision*, vol.7, no.1, pp.11–32, 1991.

[13] S. Takano, K. Niijima and T. Abdukirim, "Fast face detection by lifting dyadic wavelet filters," *Proc. of the IEEE Int'l Conf. on Image Processing (ICIP2003)*, vol.III of III, pp.893-896, 2003.

[14] S. Takano, K. Niijima and K. Kuzume, "Personal identification by multiresolution analysis of lifting dyadic wavelets", *Proc. of the 12th European Signal Processing Conference (EUSIPCO 2004)*, pp.2283-2286, 2004.